https://dx.doi.org/10.4314/ijs.v25i3.15

SYNTHESIS, CHARACTERIZATION, ANTIMICROBIAL ACTIVITIES AND COMPUTATIONAL STUDIES OF SOME CARBAMOYL PHOSPHONATES

Doherty, W. O.[1,*], Olasunkanmi, L. O.[1,3,*], Ogunkunle, O. A.[1], Akinpelu, D. A.[2] and Ojo, I. A. O.[1]

[1]Department of Chemistry, Obafemi Awolowo University, Ile-Ife, Nigeria.
[2]Department of Microbiology, Obafemi Awolowo University, Ile-Ife, Nigeria.
[3]Department of Chemical Sciences, University of Johannesburg, Doornfontein Campus, Johannesburg 2028, South Africa.
[*]Corresponding Author's Email: winstondoherty@oauife.edu.ng; loolasunkanmi@oauife.edu.ng
(Received: 23rd July, 2023; Accepted: 29th September, 2023)

ABSTRACT

Four carbamoyl phosphonates, namely diethyl *p*-tolylsulphonyl carbamoyl phosphonate (NA), dimethyl *p*-tolylsulphonyl carbamoyl phosphonate (NC), dimethyl *p*-tolyl carbamoyl phosphonate (ND) and dimethyl *p*-tolylsulphonylmethane carbamoyl phosphonate (NE) were synthesized and characterized using FTIR, ^{1}H- and ^{13}C-NMR. The products were screened *in vitro* for their growth-inhibitory activity against nine Gram-positive strains, three Gram-negative bacteria strains, and a fungus isolate. Some compounds exhibited broad-spectrum (*in vitro*) activity against the bacterial strains, and all showed activity against the only fungus used. It was observed that NC showed the highest overall activity against the microorganisms. Density functional theory (DFT) calculations conducted at ωB97XD/def2-TZVP level of theory corroborated the structural conformations of the molecules deduced from spectroscopic analyses. Predicted reactivity indices of the compounds also correlate fairly with the observed biological activities.

Keywords: Carbamoyl phosphonate, Antimicrobial activity, Organophosphorus, Broad spectrum, Reactivity indices, Density functional theory.

INTRODUCTION

Organophosphorus compounds (OPs), which consist of carbamoyl phosphonates, represent an extensively important class of chemical compounds in which organic units are bonded to a phosphorous atom or a phosphorous-based functional group [Fest and Schmidt, 1973; Demkowicz *et al*., 2016]. These compounds possess unique chemical properties and biological activities, giving them a broad spectrum of applications. OPs have been widely used in the agricultural sector as pesticides (Singh and Walker, 2006; Demkowicz *et al*., 2016; Fu *et al.,* 2022) and insecticides (Eddleston *et al*., 2005; Chambers *et al*., 2010). Their efficacy as systemic insecticides is well-established, as many exhibit remarkable selectivity towards insects.

In the industrial sectors, OPs have been reportedly used as constituents of flame retardants in plastics, textiles, and building materials, and as plasticisers, stabilisers, anti-foaming and wetting agents, as well as additives in lubricants and hydraulic fluids (Marklund *et al*., 2003). Microbiological actions of OPs were first reported at the beginning of 1940, but systematic investigations of their fungicidal and bactericidal properties began much later (Meyers *et al*., 1957).

Throughout human history, the need for food has been a crucial aspect of survival and energy. As the population grew, producing enough food to sustain it became increasingly important. However, since the dawn of civilization, efforts to produce sufficient food supplies have been hindered by the detrimental effects of insects, pests, and crop diseases. The most common pests that negatively affect crop growth include insects, fungi, and weeds. As such, the development of synthetic chemicals to combat these pests has been a topic of interest for many years (Fest and Schmidt, 1973; Sheail, 1991; Bate, 2007; Casida and Durkin, 2013; Zhang *et al*., 2017).

Pesticides were discovered in the 1940s and 1950s and became widely used in American agriculture. However, the types of pesticides used have evolved significantly since then. In the late 1950s and early 1960s, organic insecticides were popular, and organochlorines were the most widely used

class of insecticides. However, due to growing environmental concerns and regulatory legislation influenced by the publication of Silent Spring, these harsh pesticides were discontinued. Today, many organochlorine insecticides, including aldrin and dieldrin (1974), chlordane and heptachlor (1980), DDT (1982), linden (1984), and toxaphene (1982), are no longer used in the United States (Bate, 2007; Unsworth, 2010; Casida and Durkin, 2013; United States Environmental Protection Agency, 2016). These persistent, non-polar materials tend to accumulate in the fatty tissues of many wildlife species, as they are highly lipophilic. While chlorinated hydrocarbon insecticides were still utilized in some countries as of 1996, the trend has been towards safer and more sustainable alternatives (Zhang *et al*., 2011; Bernardes *et al*., 2015).

Despite the ban on chlorinated hydrocarbon insecticides in the 1980s, small amounts of these insecticides were detected in air, sediment, and water samples during the 1990s. However, the levels found were minimal. In the United States, organic herbicides have been the main type of pesticides utilized since the mid-1970s (Meyers *et al*., 1957). Organophosphate-based insecticides have an advantage in that they degrade rapidly after application, leaving no harmful residue. This distinguishes them from organochlorine insecticides, as they do not accumulate in food chains or persist in the environment. As herbicides and fungicides, OPs are growing in use and remain an important area of interest for pesticide research. However, there seems to be less emphasis on exploring new compounds within this group in recent years. It is crucial to continue researching and developing new compounds with improved antimicrobial and antifungal properties.

In this article, we report the synthesis of some carbamoyl phosphonates and their antimicrobial evaluation. Since chemical and biological activities are often traced to molecular and electronic structures, a computational study was carried out on the compounds to gain additional insights into their behaviour.

MATERIALS AND METHODS

All reagents used were of an analytical grade from BDH chemicals, and most were used without further purification. However, acetone and *n*-hexane employed in the synthesis and chromatographic purification processes were distilled with *n*-hexane dried over sodium. The standard bacteria of the National Collection for Industrial Bacteria (NCIB) and Locally Isolated Organisms (LIO) used in this work were obtained from the culture collection of Prof. D. A. Akinpelu of the Department of Microbiology, Obafemi Awolowo University, Ile-Ife, Nigeria. Melting points were determined in open capillary tubes on a Gallenkamp (variable heater) melting point apparatus. Infrared spectra were run in KBr Pellets in Buck Scientific Inc. IR Spectrophotometer model 500. ^{1}H and ^{13}C-NMR spectra were run on a Varian Mercury - 200BB NMR Spectrometer operating at 200 MHz for proton and 50 MHz for carbon-13. Chemical shifts are reported in parts per million per (ppm) relative to tetramethylsilane (TMS) as an internal standard.

Syntheses

General Protocol

To a stirred solution of phosphite and sodium in 20 mL of dry *n*-hexane, isocyanate in 10 mL dry *n*-hexane was added rapidly from a dropping funnel carrying a calcium chloride guard tube. An equal mole of phosphite, sodium and isocyanate were used in each case. The resulting mixture was left for about ten minutes and then refluxed for 2 h. After cooling and concentration, the crude samples were then purified using column chromatography with silica gel [Kieselgel 60 (70 – 230 mesh ASTM)] as the stationary phase and a gradient solvent mixture of *n*-hexane/acetone as the mobile phase.

Synthesis of Diethyl-p-*tolylsulphonyl carbamoyl phosphonate (NA)*

In this synthesis, diethyl phosphite (2.059 g, 0.0149 mol, 2 mL), sodium (0.0343 g, 0.00149 mol) and *p*-tolylsulphonyl isocyanate (2.941 g, 0.0149 mol, 2.3 mL) were used following the standard procedure earlier highlighted under anhydrous condition. After 2 h, a clear light-yellow homogenous solution resulted, which gave the desired product as a light yellow crystalline solid after the solvent had been removed. Purification was achieved by column chromatography using silica gel and gradient solvent mixture of *n*-

hexane/acetone to give diethyl *p*-tolylsulphonyl carbamoyl phosphonate (3.88 g, 78%); tlc (2.7:2.3 *n*-hexane/acetone on silica) gave a single spot R_f = 0.26; the IR spectrum (KBr disc) 3321 & 3237 cm^{-1} (O-H), 3027(=C-H), 2918(C-H), 1733 cm^{-1} (N=C-OH, weak), 1582, 1498, 1458 (C=C Aromatic), 1316 (P=O), 1158 (SO_2) 1101(C-O); δ_H ($CDCl_3$) 1.1 (CH_3, t, 3H), 1.2 (CH_3, t, 3H), 2.3 (CH_3-Ph, s, 3H), 4.0 (CH_2-O, q, 2H), 4.1 (CH_2-O, q, 2H), 7.2 (2H, m) and 7.8 (2H, m); δ_C (50MHz, $CDCl_3$) 16.6, 16.8 (H_3C-R), 21.6 (CH_3-Ph), 64.3, 64.4 (O-CH_2-R), 127, 129, 144, 142, 168 (C=O); m.p. 112–114.5 °C.

Synthesis of Dimethyl p*-tolylsulphonyl carbamoyl phosphonate (NC)*

Dimethyl phosphite (1.791 g, 0.0163 mol, 1.5 mL), sodium (0.0375 g, 0.00163 mol) and *p*-tolylsulphonyl isocyanate (3.209 g, 0.0163 mol, 2.5 mL) were used. In this case, a paste-like substance resulted. Purification was also achieved by column chromatography using silica gel and gradient solvent mixture of *n*-hexane/acetone to give dimethyl *p*-tolylsulphonyl carbamoyl phosphonate (4.47 g, 89%); tlc (3.5:1.5 *n*-hexane/acetone on silica) gave a single spot, R_f = 0.27; IR (KBr disk) 2918, 2858 (C-H), 3237, 3327 (O-H), 3117(=C-H), 1733 (N=C-OH, weak), 1582, 1462 (C=C Aromatic), 1315 (P=O), 1157 (SO_2), 1101(C-O); δ_H (200MHz, $CDCl_3$) 2.4 (CH_3-Ph, s, 3H), 3.4 (CH_3-O, s, 3H), 3.6 (CH_3-O, s, 3H), 7.3 (2H, d, J = 8 Hz), 7.8 (2H, d, J = 8 Hz) and 8.5 (N-H); δ_C (50MHz, $CDCl_3$) 20.5 (CH_3-Ph), 52.5, 52.6 (CH_3-O), 127.4, 129.6, 136.4, 140.7, 143, 145 (N=C-OH); m.p. 130 – 132 °C.

Synthesis of Dimethyl p-tolylcarbamoyl phosphonate (ND)

Dimethyl phosphite (2.267 g, 0.0206 mol, 2 mL), sodium (0.0473 g, 0.00206 mol) and *p*-tolyl isocyanate (2.743 g, 0.0206 mol, 2.6 mL) were used based on the procedure above. A paste-like substance resulted, which later solidified to give the desired products as a white crystalline solid. Purification was achieved by column chromatography using silica gel and gradient solvent mixture of n-hexane/acetone to give dimethyl *p*-tolylcarbamoyl phosphonate (3.76 g, 75%), tlc (4:1 *n*-hexane/acetone on silica) also gave single spot, R_f = 0.16; IR (KBr disc) 3247 (O-H), 3454 (N-H). 3028 (=C-H), 2949, 2852 (C-H), 1652 & 1520 (C=O str., N-H deformation called amide I and II), 1593, 1453, 1405 (C=C Aromatic). 1265 (P=O), 1040 (C-O); δ_H (200MHz, $CDCl_3$) 2.3 (CH_3-Ph, s, 3H), 3.8, 3.9 (CH_3-O, s, 3H). 7.2 (2H, d, J = 8 Hz), & 7.6 (2H, d, J = 8 Hz), 8.5 (N-H); δ_C (50MHz, $CDCl_3$) 21.2 (CH_3-Ph) 54.7, 54.8 (CH_3-O), 121.6, 129.8. 134.9. 135.6 (Aromatic C), 164.2 (C=O); m.p. 110 –111 °C.

Synthesis of Dimethyl p-tolylsulphonylmethane Carbamoyl phosphonate (NE)

Dimethyl methane phosphonate (1.99 g, 0.016 mol, 1.8 mL), sodium (0.0368 g, 0.0016 mol) and *p*-tolyl sulphonylisocyanate (3.16 g, 0.016 mol, 2.43 mL) were used. It was observed that the sodium did not dissolve in the mixture of phosphite and *n*-hexane, and the little that dissolved did not completely dissolve as quickly as it did for dialkyl phosphite. The standard procedure was followed to give the desired product as a cream crystalline solid. The product was purified by column chromatography using silica gel and gradient solvent mixture of *n*-hexane/acetone to give dimethyl *p*-tolylsulphonyl methanecarbomyl phosphonate (4.13 g, 83%); tlc (3:2 *n*-hexane/acetone on silica) gave a single spot, R_f = 0.56; IR (KBr disc) 3237 (O-H), 3327 (N-H), 3111 (=C-H), 2925, 2875 (C-H), 1727 (N=C-OH, weak), 1594, 1528, 1414 (C=C Aromatic), 1330 (P=O), 1161 (SO_2), 1083 (C-O); δ_H (200MHz, $CDCl_3$) 2.4 (CH_3-Ph, s, 3H) 2.6 (CH_2-P=O. s. 2H), 3.6, 3.7 (CH_3-O, s, 3H), 7.2 (2H, d, J = 8.4 Hz), & 7.8 (2H, d, J = 8.4 Hz); δ_C (50MHz, $CDCl_3$) 21.5 (CH_3-Ph), 32.1 (CH_2-P=O), 52.5, 52.6 (CH_3-O), 126.3, 129.0, 143.2 (Aromatic C); m.p. 141–143 °C.

Antimicrobial Sensitivity Testing of the Synthesized Compounds

In this study, we tested the antibacterial activity of the synthesised compounds using the agar well diffusion method, following standard protocols (Akinpelu, 1999). Diagnostic sensitivity test agar (Biotech Ltd) was used as the medium, and streptomycin was employed as the standard antibacterial agent at 1 mg/mL concentration. 40 g of powder was weighed and dispersed in 1 L of distilled water, and the mixture was allowed to soak for 10 min and swirled to mix before

sterilising by autoclaving. In contrast, the microorganisms used in the experiment were prepared by inoculating the bacterial isolates into nutrient broth in test tubes under aseptic conditions and incubated at 37 °C for 18 h in a Gallenkamp incubator.

Determination of Minimum Inhibitory Concentration (MIC)

The Minimum Inhibitory Concentration (MIC) was obtained using the method of Russell and Furr (1972).

Details of DFT Calculations

Molecular structures of NA, NC to NE were modelled and visualised with the aid of GaussView 5.0. The latest long-range-corrected functional from Head-Gordon and coworkers, namely ωB97XD, which includes empirical dispersion, was used for the DFT calculations (Chai and Head-Gordon, 2008). The ωB97XD functional was used together with the valence triple-zeta basis set of Ahlrichs and coworkers, def2-TZVP (Weigend and Ahlrichs, 2005; Weigend, 2006). The ωB97XD/ def2-TZVP model was employed for geometry optimisations, frequency, and natural bond orbital (NBO) calculations for all the molecules. The success of the ωB97XD/def2-TZVP model in geometry optimisations and calculation of different quantum chemical parameters for many organic molecules has been reported in the literature (Shenderovich, 2021; Balović *et al.*, 2022). All DFT calculations were conducted with the aid of Gaussian16 [Frisch *et al.*, 2016]. Full NBO analysis was obtained with the aid of the NBO program [Glendening *et al.*, 1998] embedded in Gaussian16 (as link 607), and it was invoked by using the pop=nbo keyword. All optimised structures produced non-negative vibrational frequencies, which confirmed them to be true ground-state molecular geometries.

RESULTS AND DISCUSSION

Synthesized compounds and their physical characteristics

The carbamoyl phosphonates were prepared in good yield ranging from 57% to 89%. The products prepared, and some of their physical properties are summarised in Table 1.

The presence of the polar sulphonyl group attached to the cumulative double bond system significantly increased the reactivity of the isocyanato group towards a nucleophilic attack on the central carbon atom. This was clearly demonstrated in the yield of the compounds with the desired properties and is a characteristic of sulphonyl isocyanates. The reaction of diethyl phosphite and *p*-tolylsulphonyl isocyanate produced a pure yield of diethyl *p*-tolylsulphonyl carbamoyl phosphonate (NA, 78%). Similarly, dimethyl *p*-tolylsulphonyl carbamoyl phosphonate (NC) was obtained in higher yield compared to dimethyl *p*-tolyl carbamoyl phosphonate (ND). In the reaction of dimethyl methane phosphonate with the *p*-tolylsulphonyl, the trend did not hold. However, it is reflected in the yield after purification of the crude products. Compounds NE, a sulphonyl product, was obtained in 83% yield after purification.

The compounds' spectroscopic data (IR and NMR) (*vide supra*) confirmed the structures of the synthesised carbamoyl phosphonates. The structures of the compounds, deduced from the measured spectroscopic parameters, are shown in Figure 1.

Bands in the region of 1158, 1316, 1400-1650, 3300, and 2920 cm^{-1}, typical of the SO_2, P=O, C=C aromatic, O-H, and C-H groups, respectively, were found in all the compounds. Besides the common bands, the spectra of NA established the non-equivalence of the CH_2 and CH_3 of the ethoxy group attached to P=O. The two methyl groups showed overlapping triplet at 1.2 ppm, while methylene groups showed overlapping quartet at 4.0 and 4.1 ppm in the ^{1}H NMR of the compound. ^{13}C NMR showed a similar trend with two signals of the same intensity at 16.6 & 16.8 ppm for methyl groups and 64.3 & 64.4 ppm for methylene groups. However, the signals corresponding to the aromatic nucleus and carbonyl of amide showed at the expected region for both the ^{1}H and ^{13}C NMR.

Table 1: Yield and physical properties of synthesized compounds.

Compound Code	Molecular Formula	Molecular Weight	% Yield	Melting Point ^{0}C (Uncorrected)	Colour	R_f (*n*-hexane/acetone)
NA	$C_{12}H_{18}O_6NPS$	335.32	78	112-114.5	White	0.26
NC	$C_{10}H_{14}O_6NPS$	307.26	89	130-132	White	0.27
ND	$C_{10}H_{14}O_4NP$	243.20	75	110	White	0.16
NE	$C_{11}H_{16}O_6NPS$	321.29	83	141-143	White	0.56

In addition to the common bands, NC and NE showed an N=C- double bond around 1730 $cm^{-1,}$ typical of the N=C-OH (oxime). The I.R. spectra showed very weak bands, which oximes usually give with the attendance disappearance of bands in the region of 1680 and 1570 for C=0 str. & N-H def. The fact that the carbamoyl phosphonate can exhibit keto-enol tautomerism that is typically depicted by Figure 2 would explain the disappearance of C=O str. and N-H def. in ^{13}C NMR and IR spectra of NC and NE, respectively. The N=C-OH absorption due to keto-enol tautomerism is slightly shifted to a higher wavenumber in both compounds, owing to the influence of the neighbouring polar sulphonyl group. The value in NC is higher than that of NE due to the additional contributing effect of P=O.

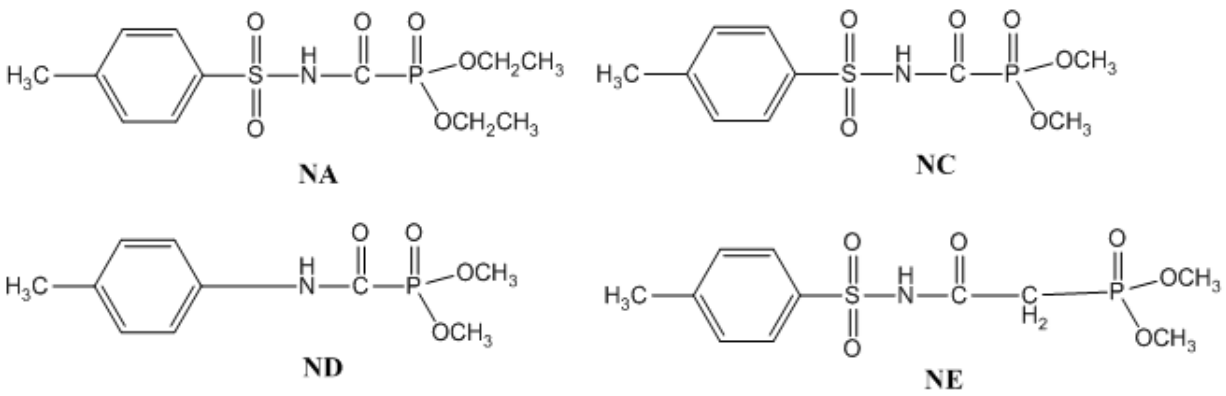

Figure 1: Molecular structures of the synthesized compounds as deduced from spectroscopic data.

Figure 2: Typical keto-enol tautomerism in carbamoyl phosphonate.

The distinguishing features in the ^{1}H and ^{13}C NMR of NC and NE is found in the CH_2 of NE, which is sandwiched between C=O and P=O. The protons of the CH_2 appeared as a singlet at 2.6 ppm in ^{1}H and the carbon at 32.1 ppm in ^{13}C NMRs. Apart from this notable distinguishing feature, the other groups gave appropriate signals at the expected regions, and their values are close due to the similarity in their structures. The expected structures of NC and NE, as deduced from the ^{1}H and ^{13}C NMR spectra, are shown in Figure 2.

It is important to note that the alkoxy group resonation in the ^{1}H and ^{13}C NMR spectra of

synthesized compounds are not equivalent. The non-equivalence of protons in organophosphorus compounds is due to stereochemical and steric factors (Hall *et al.*, 1977). The two alkoxy groups attached to phosphorus exhibit different chemical shifts and are magnetically non-equivalent. Additionally, the methylene protons of the ethyl groups (NA) and those between C=O and P=O in NE also showed peak doubling. The non-equivalence of the alkoxy groups in the synthesized compounds might be attributed to the prochiral phosphoryl phosphorus atom and the lack of free rotation, resulting in conformational strain around P=O.

Jardine and co-workers conducted a study on organophosphorus esters that had an alkoxy substituent and a benzene ring and discovered that the alkoxy groups were either located above or below the phosphorus atom, which has a nearly tetrahedral shape (Jardine *et al.*, 1969; Mentz *et al.*, 1996). This indicates that the alkoxy groups can be either close to or far from the benzene ring, depending on the rotation around the P-O-C linkage. The study showed that the preferred conformation was the up conformation, where one alkoxy group was closer to the aromatic ring while the other was farther away. Quantum chemical calculations later supported this discovery. The study also revealed that the differential diamagnetic anisotropic effect caused the chemical shifts of the groups to differ in both monomers and dimers due to the presence of an aromatic ring in the molecular structure. It's worth noting that this effect could also be a contributing factor for both methylene protons and alkoxy groups. Although non-equivalence has been reported in compounds without an aromatic ring or a formal asymmetric centre (Henry *et al.*, 2015; Eills *et al.,* 2017), the study found that intrinsic term, conformational population differences, and steric factors played important roles in most cases.

The IR, ^{1}H, and ^{13}C NMR of compound ND (dimethyl *p*-tolyl carbamoyl phosphonate) confirmed the expected structure (also shown in Figure 1). The two methyl groups of the methoxy in the structure were also found not to be equivalent both in ^{1}H and ^{13}C NMR. The stretching vibrations at 1652 cm^{-1} & 1520 cm^{-1} in the infrared spectrum of this compound are bands of C=O str. and N-H def. of amide, usually referred to as amide 1 & II. This characteristic feature is typical of carbonyl of amide, and the two bands are generally of about the same intensity, evidenced in this compound's IR spectrum. Both ^{1}H and ^{13}C NMR confirmed this pattern. In the ^{1}H NMR of this compound, the methoxy protons appeared at 3.8 & 3.9 ppm and showed the non-equivalence of the two methoxy groups. This trend was also sustained in the ^{13}C NMR spectrum, where the two methoxy carbons appear at 54.7 and 54.8 ppm.

The signals corresponding to CH_3-Ph and aromatic protons showed at the expected region in the ^{1}H and ^{13}C NMR. It is worthy of note that all the synthesized compounds reflected the features of the *p*-tolyl nucleus both in the IR and NMR spectra, and the infrared spectra showed characteristic absorptions attributed to P=O (1390-1370) and SO_2 (1190-1180 cm^{-1}).

The possible reaction mechanism for carbamoyl phosphonate formation using sodium as a catalyst is shown in Scheme 1.

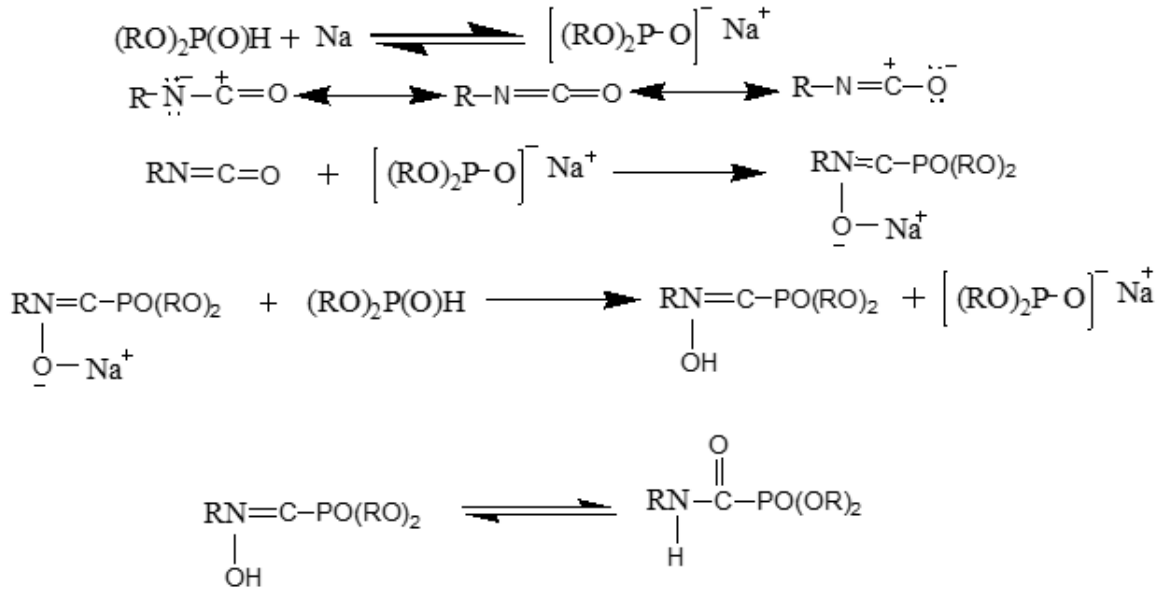

Scheme 1: Possible reaction mechanism for the formation of carbamoyl phosphonate in the presence of sodium catalyst.

Antimicrobial Activity

The synthesized compounds (NA, NC– NE) were screened *in vitro* for possible antibacterial activity, using the solvent (DMSO) as a negative control and streptomycin as the reference antibiotics. The solvent showed negligible activity against test organisms, thus establishing that the activities recorded were those of the titled compounds. The results as presented in Table 2 indicated that the compounds generally showed a broad-spectrum of activity against the bacterial strain.

NA and NC showed activities against seven out of the nine Gram-positive bacterial strains tested, while ND and NE showed activities against six Gram-positive bacteria. Meanwhile, all the compounds showed activities against five of the nine Gram-positive bacterial strains in common. NA and NC did not show activities against *Bacillus polymyxa* (LIO), ND did not show activities against *Bacillus polymyxa* (LIO) and *Bacillus anthracis* (LIO), while NE did not show activities against *Bacillus anthracis* (LIO) and *Streptococcus faecalis*. Streptomycin, which was used as the reference standard, showed activity against all the nine bacteria species. On the other hand, for the Gram-negative bacterial strains, all the compounds (except for NA) showed activities against *Klebisiella pneumonia* and *Escherichia coli*, except NA, which did not show activity against *Escherichia coli*. Their zones of inhibition range from 12 mm to 20 mm, with compound NE showing the largest zone of inhibition (20 mm observed for *Klebisiella pneumonia*). Whereas streptomycin, which was used as standard, showed no activity against the *Klebisiella pneumonia* and *Escherichia coli*. A simple trend could not be generated for the degree of activities of the compounds against the Gram-positive bacterial strains. All the compounds are active against the only fungus used [*Candida albicans* (LIO)], with NA and NE showing the largest zones of inhibition (16 mm).

The minimum inhibitory concentration (MIC) of the synthesized compounds was determined for Gram-positive and Gram-negative bacteria, and the results are shown in Table 3.

Table 2: Result of the antimicrobial screening (sensitivity testing) on Gram-positive and Gram-negative bacteria, with zone of inhibition in mm (compounds conc. = 2 mg/mL, Str = 1 mg/mL).

Compound Code/ Microorganisms	NA	NC	ND	NE	Str
Gram-positive Bacteria					
Corynebacterium pyogenes (LIO)	0	0	0	0	20
Bacillus polymyxa (LIO)	0	0	0	12	15
Bacillus stearothermophilus	16	17	20	20	23
Bacillus siibtilis	15	16	18	17	20
Bacillus anthracis (LIO)	12	14	0	0	18
Streptococcus fuecalis	14	14	10	0	23
Bacillus aureus	12	20	21	20	28
Staphylococcus aureus	15	13	12	15	21
Clostridium sporogenes	16	16	14	20	25
Gram-negative Bacteria					
Pseudomonas fluorescens	0	0	0	15	30
Klebisiella pneumonia	0	12	12	20	0
Escherichia coli	14	14	12	13	0
Candida albicans (LIO)	16	13	14	16	ND

Str = Streptomycin ND = not detected

The MIC of the compounds varied between 31 μg/mL and 500 μg/mL for all strains. The MIC of the reference standard streptomycin varied between 7.8 μg/mL and 500 μg/mL. NC and ND showed similar MIC to streptomycin (31 μg/mL) against *Bacillus cereus*. NE showed lower MIC than streptomycin against *Bacillus stearethermophilus*. NA and NE showed lower MIC than streptomycin against *Staphylococcus aureus*. On a general note, compound NC had the highest activity, while all the compounds had better activity than the standard streptomycin, especially on Gram-negative bacterial and fungal strains.

Table 3: Result of minimum inhibitory concentration (MIC) test of compounds in (mg/mL) on various Gram-positive and Gram-negative bacteria.

Compound Code/ Microorganisms	NA	NC	ND	NE	Streptomycin
Gram-positive Bacteria					
Bacillus polymyxa (LIO)	-	-	-	1.0	0.125
Bacillus subtilis	0.125	0.125	0.125	0.125	0.0625
Bacillus anthracis (LIO)	0.500	0.250	-	-	0.0313
Bacillus cereus	0.500	0.0313	0.0313	0.125	0.0313
Bacillus stearethermophilus	0.125	0.0625	0.0625	0.0313	0.0625
Streptococcus faecalis	0.250	0.250	0.500	-	0.0625
Staphylococcus aureus	0.125	0.500	0.500	0.250	0.500
Clostridium sporogenes	0.0625	0.0625	0.250	0.0313	0.0078
Gram_negative Bacteria					
Pseudomonas flourescens	-	-	-	0.250	0.250
Klebsiella pneumoniae	-	0.500	0.500	0.0625	-
Escherichia coli	0.250	0.250	0.500	0.500	-
Pseudomonas aeruginosa	-	-	-	0.500	0.250

Molecular and Electronic Structures from DFT Calculations

Optimised structures of the studied compounds are shown in Figure 3, listing salient bond lengths between atoms. For selected interatomic bond distances in the optimised molecular structures, P=O range from 1.4560 Å to 1.4646 Å, and C=O range from 1.2065 Å to 1.2141 Å (NA to ND), except for NE in which C=O bond is relatively longer (1.4615 Å) due to its separation from P=O group by a methylene group. All the bond distances are within the usual ranges reported in the literature for the same bonds in similar compounds, either as isolated ligands or complexes (Conary *et al.*, 1991; Conary *et al.*, 1993; Breuer, 1996; Brovarets *et al.*, 2018; Van der Weide *et al.*, 2019). As observed from the spectroscopic data, especially NMR results, the two alkoxy groups attached to the phosphorus atom are nearly at opposite sides of the P=O plane such that one alkoxy group is oriented towards the phenyl group while the other is farther away. In other words, the alkoxy groups are in different chemical environments and are not expected to behave chemically the same. The dihedral angles around the C-O groups relative to the P=O functional group are ca. 96.05°, 98.57°, 66.57° and 76.43° for NA, NC, ND, and NE, respectively. Considering the structural difference between NC and ND, it could be assumed that the sulphonyl group present in NC was responsible for a larger torsion angle between the two methoxy groups compared to ND. The intermediate methylene (-CH_2) group between P=O and C=O in NE compared to NC is also responsible for a lower torsion angle between the planes of methoxy groups. The bond lengths of P=O are in the order ND > NE > NA > NC, suggesting that the P=O bond order decreases with an increasing chain length of the alkoxy group (cf. NA and NC), while the sulphonyl group could be regarded as bond strengthening for the P=O as its absence in ND reduced the P=O bond order. Furthermore, the electron-withdrawing effect of the amide C=O on the P=O in NE was lessened by the adjoining -CH_2 group, resulting in a slightly stronger P=O bond compared to ND.

The effects of both sulphonyl and -CH_2 groups as may apply to each compound could also be seen on the bond lengths of amide the C=O, which decrease with increasing electron-withdrawing effect. The C-O bonds of the alkoxy groups generally exhibit different bond lengths due to their appearance in different chemical environments, as already observed in the NMR data.

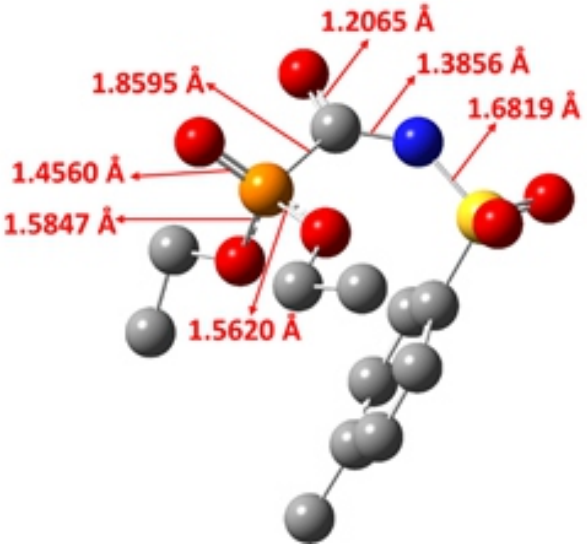

NA

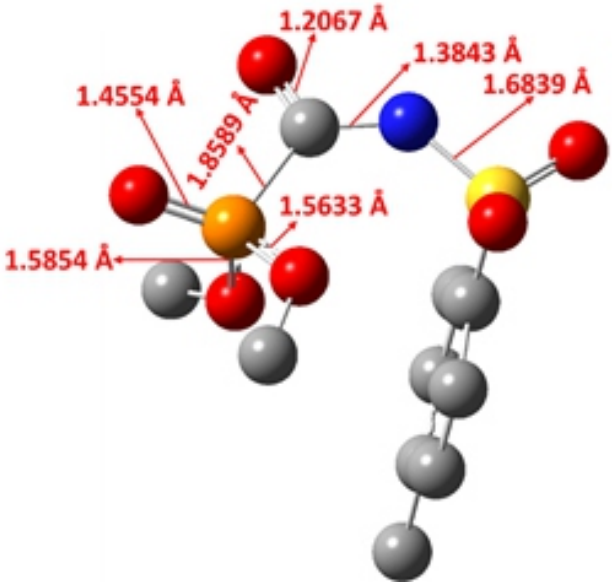

NC

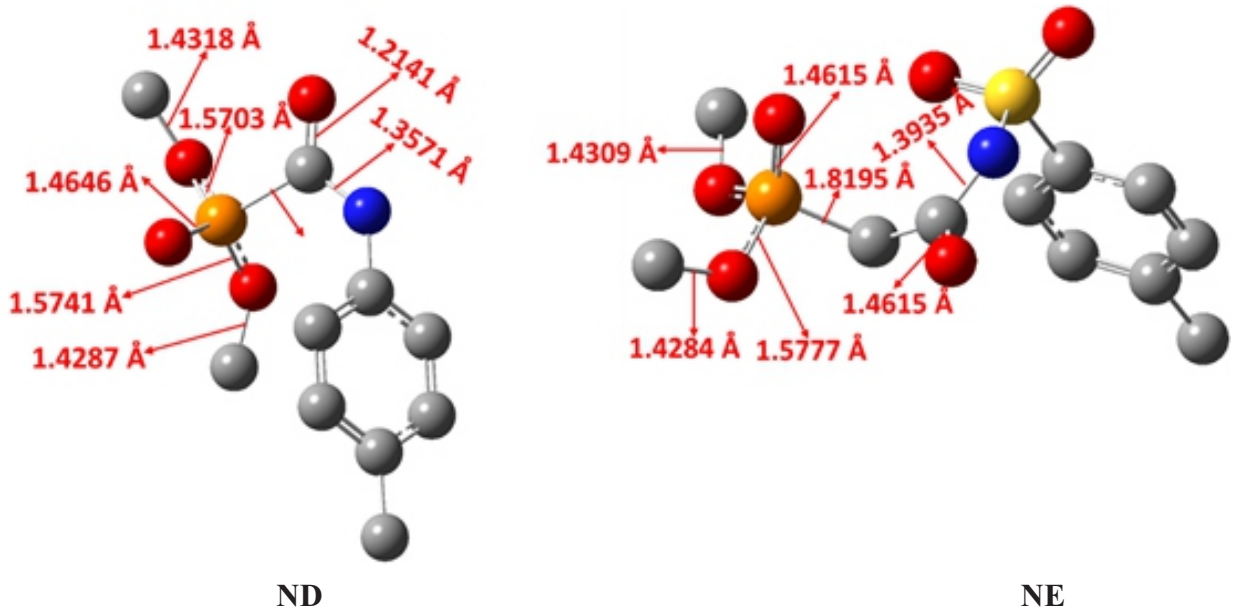

Figure 3: Optimised Structures of the studied compounds obtained at ωB97XD/def2-TZVP level of theory.

It was further observed that the C-O group that is closer to the phenyl ring is stronger than its counterpart that is farther away in the same compound. This might be due to non-covalent interactions between the aromatic pi-system and the nearby alkoxy group (Newberry and Raines, 2017). Contour maps of frontier molecular orbitals (FMOs), the highest occupied molecular orbital (HOMO), and the lowest unoccupied molecular orbital (LUMO) are shown in Figure 4. The contour maps visualised at 0.02 isovalue reveal that both the HOMO and LUMO electron density are delocalised over the aromatic ring and extended to the sulphonyl and amide functional groups.

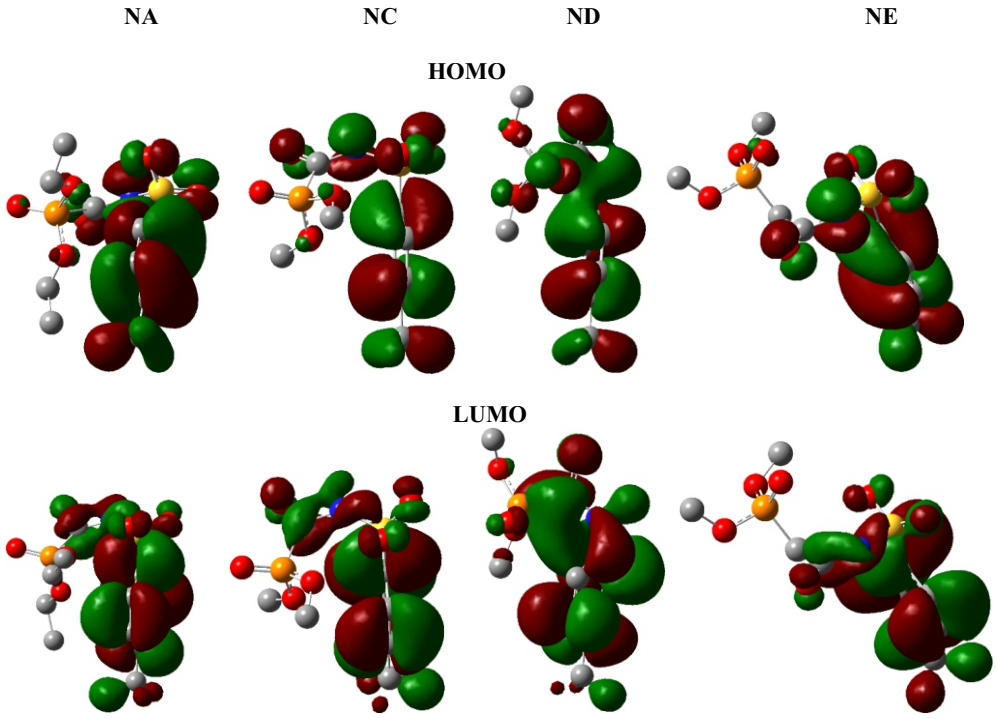

Figure 4: HOMO and LUMO contour maps of the studied compounds visualised at 0.0200 isovalue.

Some reactivity indices of the compounds were calculated using previously reported mathematical relations. The reactivity indices, formulas, and values are listed in Table 4. The reactivity indices were calculated as reported elsewhere (Sasikumar *et al.*, 2015; Olasunkanmi *et al.*, 2016; Gázquez *et al.*, 2017). The values of the highest occupied molecular orbital energy (E_{HOMO}), which is an index of the electron-donating ability of the molecules, are in the order ND > NE > NA > NC, which also correlates with the order of electron-donating power (ω^-). This suggests that ND is the most reactive of the four compounds towards an electrophile, while NC is the least reactive towards an electrophile. On the other hand, NC has the highest global electron-withdrawing power (ω^+) and highest net electrophilicity, which suggests the highest chemical reactivity towards a nucleophile. This is also in agreement with the observed relative potency of biological activities of the molecules in which NC showed the overall highest activity.

Table 4: Reactivity indices of the studied compounds.

Reactivity Index, Symbol, Unit	Formula	NA	NC	ND	NE
Energy Gap (ΔE, eV)	$\Delta E = E_{LUMO} - E_{HOMO}$	9.705	9.717	9.656	9.753
Ionisation Potential (I, eV)	$I = -E_{HOMO}$	9.554	9.565	8.741	9.522
Electron Affinity (A, eV)	$A = -E_{LUMO}$	-0.151	-0.152	-0.915	-0.231
Chemical Potential (μ, eV)	$\mu = -\frac{1}{2}(I + A)$	-4.702	-4.707	-3.913	-4.645
Global Hardness (η, eV)	$\eta = \frac{1}{2}(I - A)$	4.702	4.707	3.913	4.645
Global Softness (σ, eV)	$\sigma = \frac{1}{\eta}$	0.213	0.212	0.256	0.215
Global Electronegativity (χ, eV)	$\chi = \frac{1}{2}(I + A)$	4.853	4.858	4.828	4.876
Electrophilicity (ω, eV)	$\omega = \frac{\mu^2}{2\eta}$	2.351	2.353	1.957	2.323
Global Electron Donating Power (ω^-, eV)	$\omega^- = \frac{(3I + A)^2}{16(I - A)}$	5.235	5.241	4.146	5.145
Global Electron Withdrawing Power (ω^+, eV)	$\omega^+ = \frac{(I + 3A)^2}{16(I - A)}$	0.533	0.534	0.233	0.500
Net Electrophilicity ($\omega^\pm$, eV)	$\omega^\pm = \omega^+ + \omega^-$	5.768	5.774	4.379	5.645
Dipole Moment (Debye)	-	7.386	7.325	4.016	6.441

CONCLUSION

Diethyl-*p*-tolylsulphonyl carbamoylphosphonate (NA), dimethyl *p*-tolylsulphonyl carbamoyl phosphonate (NC), dimethyl-*p*-tolyl carbamoyl phosphonate (ND) and dimethyl-*p*-tolylsulphonylmethane carbamoyl phosphonate (NE) have been successfully synthesised by the reaction of alkyl phosphite and *p*-tolylsulphonyl isocyanate (*p*-tolyl isocyanate in the case of ND). FTIR, ^{1}H- and ^{13}C-NMR confirmed the structures of the synthesized compounds. Spectroscopic analyses are supported by quantum chemical calculations. The compounds showed *in vitro* antimicrobial activity against Gram-positive and Gram-negative bacteria as well as a fungus isolate, with NC showing the highest average activity. Quantum chemically derived reactivity indices, especially the net electrophilicity, suggested that NC is the most reactive of the four compounds towards a nucleophilic centre, and the trends of some of the reactivity indices correlated with the experimental biological activity data.

ACKNOWLEDGEMENTS

W.O.D and I.A.O.O acknowledge the Central Science Laboratory, Obafemi Awolowo University, Ile-Ife, Nigeria, for the running of ^{1}H- and ^{13}C-NMR and the Department of Chemistry, Obafemi Awolowo University, Ile-Ife, Nigeria for the running of IR spectroscopic. L.O.O.

acknowledges the Centre for High-Performance Computing (CHPC), Cape Town, South Africa, for providing access to resources for DFT calculations.

CONFLICT OF INTEREST

The authors declare that there are no competing financial interests or otherwise against the publication of the work reported herein.

REFERENCES

Akinpelu, D. 1999. Antimicrobial activity of the crude extract of Vernonia amygdalina leaves. *Fitoterapia*, 71: 75.

Aspelin, A.L. 1997. Pesticides industry sales and usage: 1994 and 1995 market estimates. Biological and Economic Analysis Division, Office of Pesticide Programs.

Balović, J., Ćoćić, D., Đorđević, S., Radenković, S., Eldik, R. V. and Pucht, R. 2022.A theoretical mechanistic study of [K⊂[2.2.2]]+ enantiomerization. *Journal of Physical Organic Chemistry*, 35(2): e4289. doi: 10.1002/poc.4289

Bate R. The rise, fall, rise, and imminent fall of DDT. American Enterprise Institute for Public Policy Research, 2007 14 (4): 1–9.

Bernardes, M.F.F., Pazin, M., Pereira, L.C. and Dorta, D.J. 2015. Toxicology Studies—Cells, Drugs and Environment. IntechOpen; London, UK: Impact of Pesticides on Environmental and Human Health; pp. 195–233.

Breuer, E. 1996. Acylphosphonates and their Derivatives. *The Chemistry of Organophosphorus Compounds*, 4: 653-729.

Brovarets, V. S., Golovchenko, O. V., Rusanov, E. B. and Rusanova, J. A. 2018.Crystal structure of diethyl {2, 2, 2-trichloro-1-[2-(1,3-dioxo-2,3-dihydro-1*H*-isoindol-2-yl)-4-methylpentanamido]ethyl} phosphonate. *Acta Crystallographica Section E: Crystallographic Communications*, 74(7): 915-917. doi: 10.1107/S20 56989018008277

Casida J.E. and Durkin K.A. 2013. Anticholinesterase insecticide retrospective. *Chemico-Biological Interactions*, 203 (1): 221–225.

Chai, J.-D. and Head-Gordon, M. 2008. Long-range corrected hybrid density functionals with damped atom–atom dispersion corrections. *Physical Chemistry Chemical Physics*, 10(44): 6615-6620.

Chambers, J.E., Meek, E.C. and Chambers, H.W. 2010. The metabolism of organophosphorus insecticides, in Hayes' Handbook of Pesticide Toxicology, *Elsevier*. p. 1399-1407.

Conary, G. S., McCabe, D. J., Meline, R. L., Duesler, E. N., Paine, R. T. Synthesis and coordination chemistry of trifunctional carbamoyl-bis-phosphonate alkane ligands. Inorganica chimica acta, 1993. 203(1): p. 11-19. doi:10.1016/S0020-1693(00)82898-4.

Conary, G. S., Meline, R. L., Caudle, L. J., Duesler, E. N. and Paine, R. T. 1991. Synthesis of bifunctional phosphonates and phosphine oxides. Structural studies of 1-*N*,*N*-diethyl-carbamoyl-2-(4-hydroxylbenzene)-ethyl phosphonic acid and diphenyl [1-(*N*,*N*-diethyl-carbamoyl)-2-(phenyl) ethyl] phosphine oxide uranyl nitrate. *Inorganica Chimica Acta*, 189(1): 59-66. doi: 10.1016/S0020-1693(00)80390-4

Demkowicz, S., Rachon, J., Daśkoa, M. and Koza, W. 2016. Selected organophosphorus compounds with biological activity: Applications in medicine. *RSC Advances*, 6(9): 7101-7112. doi: 10.1039/C5RA25446A

Eddleston, M., Eyer, P., Worek, F., Mohamed, F., Senarathna, L., von Meyer, L., Juszczak, E., Hittarage, A., Azhar, S., Dissanayake, W., Sheriff, M.H., Szinicz, L., Dawson, A.H. and Buckley, N.A. 2005. Differences between organophosphorus insecticides in human self-poisoning: a prospective cohort study. *The Lancet*, 366(9495): 1452-1459. doi: 10.1016/S0140-6736(05)67598-8

Eills, J., Blanchard, J. W., Bougas, L., Kozlov, M. G., Pines, A. and Budker, D. 2017. Measuring molecular parity nonconservation using nuclear-magnetic-resonance spectroscopy. Physical Review A, 96(4): 042119.

Fest, C. and Schmidt, K. 1973. The chemistry of organophosphorus pesticides Springer-Verlag. Berlin Heidelberg New York, p. 20.

Frisch, M. J., Trucks, G. W., Schlegel, H. B., Scuseria, G. E., Robb, M. A., Cheeseman, J. R., Scalmani, G., Barone, V., Petersson, G. A., Nakatsuji, H., Li, X., Caricato, M., Marenich, A. V., Bloino, J., Janesko, B. G., Gomperts, R., Mennucci, B., Hratchian, H. P., Ortiz, J. V., Izmaylov, A. F., Sonnenberg, J. L., Williams-Young, D., Ding, F., Lipparini, F., Egidi, F., Goings, J., Peng, B., Petrone, A., Henderson, T., Ranasinghe, D., Zakrzewski, V. G., Gao, J., Rega, N., Zheng, G., Liang, W., Hada, M., Ehara, M., Toyota, K., Fukuda, R., Hasegawa, J., Ishida, M., Nakajima, T., Honda, Y., Kitao, O., Nakai, H., Vreven, T., Throssell, K., Montgomery, J. A., Jr., Peralta, J. E., Ogliaro, F., Bearpark, M. J., Heyd, J. J., Brothers, E. N., Kudin, K. N., Staroverov, V. N., Keith, T. A., Kobayashi, R., Normand, J., Raghavachari, K., Rendell, A. P., Burant, J. C., Iyengar, S. S., Tomasi, J., Cossi, M., Millam, J. M., Klene, M., Adamo, C., Cammi, R., Ochterski, J. W., Martin, R. L., Morokuma, K., Farkas, O., Foresman, J. B., Fox, D. J. 2016. Gaussian 16, Revision C.01., Gaussian, Inc., Wallingford CT.

Gázquez, J.L., Cedillo, A. and Vela, A. 2007. Electrodonating and electroaccepting powers. The Journal of Physical Chemistry A, 111(10): 1966-1970.

Glendening, E. D., Reed, A. E., Carpenter, J. E. and Weinhold, F. NBO Version 3.1, TCI, University of Wisconsin, Madison, 1998.

Hall, C. D., Robert Ardrey, Robert Dyer and Paul G. Le Gras 1977. Magnetic non-equivalence in organophosphorus esters. *Journal of the Chemical Society, Perkin Transactions*, 2(10): 1232-1237. doi: 10.1039/P29770001232

Henry, B., Gizzi, P. and Delpuech, J.-J. 2015. Magnetic non-equivalence and dynamic NMR of *N*-methylene protons in a Histamine-containing pseudopeptide: Alanyl-Glycyl-Histamine. *Tetrahedron*, 71(36): 6227-6244.

Fu, H., Tan, P., Wang, R., Li, S., Liu, H., Yang, Y. and Wu, Z. 2022. Advances in organophosphorus pesticides pollution: Current status and challenges in ecotoxicological, sustainable agriculture, and degradation strategies. *Journal of Hazardous Materials*, 424: 127494. doi: 10.1016/j.jhazmat.2021.127494

Jardine, R., Gray, A. and Reesor, J. 1969. Peak doubling in the nuclear magnetic resonance spectra of certain phosphorus esters. *Canadian Journal of Chemistry*, 47(1): 35-41.

Marklund, A., Andersson, B. and Haglund, P 2003. Screening of organophosphorus compounds and their distribution in various indoor environments. *Chemosphere*, 53(9): 1137-1146.

Mentz, M., Modro, T. A., Koch K. R. and van Rooyen, P. H. 1996. Magnetic non-equivalence in phosphate esters. Solvent effects on the ^{1}H NMR spectrum of dibenzyl 2-pyridylphosphate. *Journal of molecular structure*, 380(1-2): 125-131. doi: 10.1016/0022-2860(95)09208-0

Meyers, D., Kemp, A., Tol, I. and Longe, M., 1957. Studies on ali-esterases 6-selective Inhibitors of the esterases of brain and saprophytic mycobacteria. *Biochemistry Journal* 65: 232 – 241.

Newberry, R. W. and Raines, R. T. 2017. The n→ π* Interaction. *Accounts of Chemical Research*, 50(8): 1838-1846.

Olasunkanmi, L.O., Kabanda, M.M. and Ebenso, E.E. 2016. Quinoxaline derivatives as corrosion inhibitors for mild steel in hydrochloric acid medium: Electrochemical and quantum chemical studies. *Physica E: Low-dimensional Systems and Nanostructures*, 76: 109-126.

Sasikumar, Y., Adekunle, A. S., Olasunkanmi, L. O., Bahadur, I., Baskar, R., Kabanda, M. M., Obot, I. B., Ebenso, E. E. 2015. Experimental, quantum chemical and Monte Carlo simulation studies on the corrosion inhibition of some alkyl imidazolium ionic liquids containing tetrafluoroborate anion on mild steel in acidic medium. *Journal of Molecular Liquids*, 211: 105-118. doi:10.1016/j.molliq.2015.06.052.

Sheail, J. 1991. Innovation and Environmental Risks. Belhaven Press; London, UK. The regulation of pesticides use: An historical perspective; pp. 38–46.

Shenderovich, I.G. 2021. Experimentally Established Benchmark Calculations of ^{31}P NMR Quantities. *Chemistry-Methods*, 1(1): 61-70.

Singh, B. K. and Walker, A. 2006. Microbial degradation of organophosphorus compounds. *FEMS microbiology reviews*, 30(3): 428-471.

United Nations Environment Programme. Stockholm Convention: Protecting health and the environment from persistent organic pollutants.

United States Environmental Protection Agency. DDT: A brief history and status. 2016,

Unsworth J. History of Pesticide Use. 2010 IUPAC-International Union of Pure and Applied Chemistry, Mai. Available online: http://agrochemicals.iupac.org/index.php?option=com_sobi2&sobi2Task=sobi2Details&catid=3&sobi2Id=31.

Van der Weide, A.I., Staples, R.J. and Biros, S.M. 2019. Crystal structures of two bis-carbamoylmethylphosphine oxide (CMPO) compounds. *Acta Crystallographica Section E: Crystallographic Communications*, 75(7): 991-996.

Weigend, F. and Ahlrichs, R. 2005. Balanced basis sets of split valence, triple zeta valence and quadruple zeta valence quality for H to Rn: Design and assessment of accuracy. *Physical Chemistry Chemical Physics*, 7(18): 3297-3305.

Weigend, F., Accurate Coulomb-fitting basis sets for H to Rn. *Physical Chemistry Chemical Physics*, 2006. 8(9): 1057-1065.

Zhang, K., Zhang, B.-Z., Li, S.-M., Zeng, E.Y. 2011. Regional dynamics of persistent organic pollutants (POPs) in the Pearl River Delta, China: Implications and perspectives. *Environ. Pollut.* 159:2301–2309. doi: 10.1016/j.envpol.2011.05.011.

Zhang, Q., Xia, Z., Wu, M., Wang, L. and Yang, H. 2017. Human health risk assessment of DDTs and HCHs through dietary exposure in Nanjing, China. *Chemosphere*, 177:211–216. doi: 10.1016/j.chemosphere.2017.03.003.